Statically Balanced Brakes

Michiel Plooij*, Tom van der Hoeven, Gerard Dunning and Martijn Wisse

** Corresponding author*
Delft University of Technology
Mekelweg 2
2628 CD Delft
The Netherlands
m.c.plooij@tudelft.nl

Abstract

Conventional brakes require a powerful actuator, leading to large, heavy and in most cases energy consuming brakes. This paper introduces a fundamentally different brake concept called statically balanced brakes (SBBs). SBBs do not require any actuation force to maintain a braking torque and only have to move a small mass to vary that torque. Therefore, their energy consumption is potentially very low. In an SBB, one of the two friction surfaces is connected through springs to a braking block. This braking block is connected through a mechanism to a second set of springs, the other side of which connects to the ground. The total energy in the two sets of springs is constant, which results in a zero-force characteristic at the braking block. The position of this statically balanced braking block determines the displacement of the first set of springs and thus the normal force between the friction surfaces. We categorize mechanisms that can be used in SBBs and show two embodiments: one with leaf springs with a range of positions with negative stiffness and one with torsion springs and a non-linear cam mechanism. Results show that the actuation force can be reduced by approximately 95-97% in comparison to regular brakes. This shows that in SBBs, the actuation force can be almost eliminated and thus showing the potential of SBBs to be small, lightweight and energy efficient.

Keywords: Brake design, statically balanced, locking mechanism, clutch

1. Introduction

Conventional brakes require a powerful actuator that generates a normal force between two friction surfaces [1, 2]. The amplitude of the normal force, the friction coefficient and the geometry of the brake together determine the braking torque. There are applications in which powerful actuators are undesired due to size and weight limitations or their (potentially high) energy consumption. Therefore, researchers have worked on designing brakes that require less actuation force.

Research on the reduction of the required actuation force can be split into three categories, that are also described in the recent review paper on locking mechanisms [3]. Firstly, self-engaging brakes have been developed that use the relative motion between the friction surfaces to pull the friction surfaces together and thereby reducing the required actuation force [4, 5, 6, 7]. Disadvantages of such brakes are that they only work in one braking direction and that they can only disengage in the opposite direction of engagement. Secondly, spring brakes (also called safety brakes or parking brakes) use a spring to keep the brake engaged without actuation force [2, 8, 9, 10]. However, these brakes still require an actuation force to keep the brake disengaged. This is solved in the third category: bi-stable brakes [11, 12]. Such brakes have a bi-stable element (e.g. a bi-stable spring), providing the brake with two stable states: the engaged state and the disengaged state. However, switching between these two states still requires a high actuation force.

Other researchers focused on implementing actuators with a high force density and a low energy consumption. The best example of this is piezo-actuated brakes [13, 14, 15, 16, 17]. Because of their high force density and low energy consumption, they are potentially very effective in solving the issues mentioned above. However, they require high voltages (that might not be available), very precise manufacturing (since they have a very small stroke) and are expensive. Furthermore, the brake construction has to be very stiff, otherwise the construction will deform, which reduces the effectiveness of piezoelectric actuators.

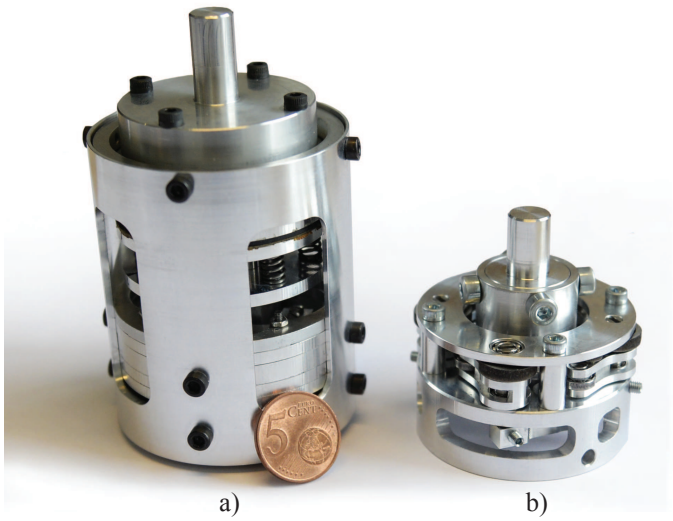

Figure 1: A picture of the two prototypes of statically balanced brakes. a) A prototype with leaf springs with a range of positions with negative stiffness. b) A prototype with torsion springs and a rotational cam mechanism.

The problem with the state-of-the-art brakes is that the actuator has to be able to generate a force equal to the normal force between the friction plates. The goal of this paper is to introduce a brake concept in which the normal force and the actuation force are decoupled. This concept potentially reduces the actuation force by 100 %.

This new brake concept is fundamentally different from current brake concepts and is called statically balanced brakes (SBBs, see Fig. 1). SBBs do not require an actuation force to hold a certain braking torque and only require a small actuation force to vary that torque. Furthermore, with small adjustments, SBBs can be changed to incorporate any of the three different functionalities mentioned above (i.e. regular-, spring- and bi-stable behavior), while still only requiring a small actuation force. Statically balanced mechanisms have also been used amongst others for intrinsically safe robotic arms [18, 19], exoskeletons [20], prostheses [21] and micro and precision mechanisms [22, 23].

The rest of this paper is structured as follows. First, section 2 explains the

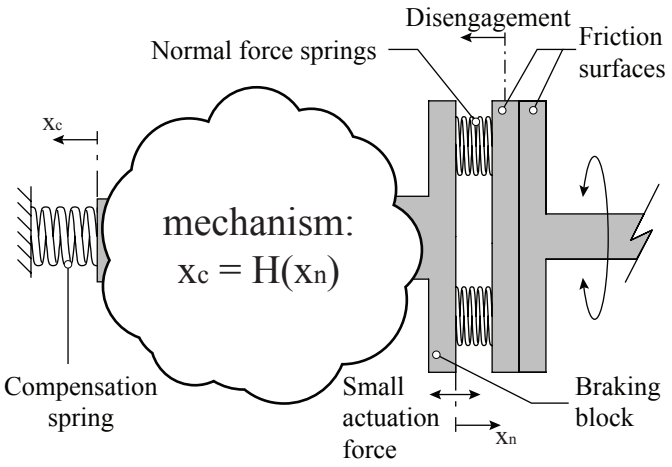

Figure 2: A schematic drawing of a statically balanced brake. The right friction surface is connected to a joint that has to be braked. The left friction surface is connected through the normal force springs with the braking block. A mechanism connects the braking block with the compensation springs and the other side of the compensation springs connects to the ground. This mechanism is visualized by the mechanism equation $x_c = H(x_n)$, that gives the relationship between the positions of the two sides of the mechanism. The position of the braking block determines the normal force between the friction surfaces.

concept of SBBs in more detail. Then, section 3 categorizes all possible embodiments of SBBs that are relatively simple and therefore small and lightweight. Sections 4 and 5 then show two prototypes of SBBs and their performance. Those results will show that the actuation forces in the prototypes are reduced by 95-97%. Finally, the paper ends with a discussion in section 6 and a conclusion in section 7.

2. The concept of statically balanced brakes

In this section we explain the concept of SBBs in more detail. First, we give a general formulation without assuming linear springs. Then, we work out the equations for a system with linear springs. Fig. 2 shows a schematic drawing of the concept of a SBB and Fig. 3 shows the working principle of a SBB for linear springs. The brake is engaged by pushing the two friction surfaces against

each other. The friction between the surfaces is assumed to be a Coulomb type friction:

$$|F_f|_{max} = \mu F_n \tag{1}$$

where μ is the Coulomb friction coefficient, $|F_f|_{max}$ is the maximum absolute friction force before the surfaces start to slip and F_n is the normal force. The brake in Fig. 2 is statically balanced by two groups of springs. The group of normal force springs is placed between the braking block and the left friction surface. The energy in this group of springs is equal to $E_n(x_n)$, with x_n being the displacement of the springs as shown in Fig. 2. The force in these springs (F_n) is equal to the normal force between the friction surfaces. Multiplying F_n by the effective radius r of the brake, gives the braking torque:

$$|T|_{max} = \mu F_n r = \mu \frac{\partial E_n(x_n)}{\partial x_n} r \tag{2}$$

This means that the position of the braking block determines the amplitude of the braking torque. Now if this were the only group of springs, an actuator would still have to generate the force F_n to hold the braking block in a certain position. In order to decouple this normal force from the actuation force, a second spring system is used: the compensation springs. The compensation springs are placed between the ground and a mechanism that also connects to the braking block. This mechanism is depicted in Fig. 2 as a cloud with the mechanism equation $x_c = H(x_n)$. This equation assumes that the overall mechanism has one degree of freedom (DOF). In section 3, we will zoom in on this part and discuss possible mechanisms. Here we will analyse the static balance of mechanisms from an energy perspective. The energy in the group of compensation springs is $E_c(x_c)$ with x_c being the displacement of the springs as shown in Fig. 2. Now the system is statically balanced when $E = E_n + E_c$ is constant for all positions of the system. The transfer ratio h from the normal force springs to the compensation springs at position x_n is equal to:

$$h(x_n) = \frac{\partial H(x_n)}{\partial x_n} = \frac{\partial x_c}{\partial x_n} \tag{3}$$

We can now write the condition for static balance as

$$\frac{\partial E}{\partial x_n} = 0 \tag{4}$$

$$\frac{\partial E_n(x_n)}{\partial x_n} + \frac{\partial E_c(x_c)}{\partial x_c} h(x_n) = 0 \tag{5}$$

Now given the two spring characteristics, this system is statically balanced for all x_n for which it holds that

$$h(x_n) = -\frac{\partial x_c}{\partial E_c(x_c)} \frac{\partial E_n(x_n)}{\partial x_n} \tag{6}$$

The force that the compensation spring applies on the braking block can be expressed as:

$$F_c = \frac{\partial E_c}{\partial x_n} = \frac{\partial E_c(x_c)}{\partial x_c} h(x_n) = -\frac{\partial E_n(x_n)}{\partial x_n} = -F_n \tag{7}$$

It is logical that $F_c = -F_n$ because this results in force equilibrium, which is another way to consider static balancing. Now assume that both the normal force springs and the compensation springs are linear:

$$E_n = \frac{1}{2} k_n \max(x_n, 0)^2 \tag{8}$$

$$E_c = \frac{1}{2} k_c x_c^2 \tag{9}$$

where k_n and k_c are spring stiffnesses and the max operator returns the maximum value of the two inputs and models the disengagement of the friction surfaces. Eq. (6) now becomes:

$$h(x_n) = -\frac{k_n \max(x_n, 0)}{k_c x_c} \tag{10}$$

From Eq. (10) it follows that $h(x_n \leq 0) = 0$. This means that the mechanism is in a singular position or that the mechanism contains a clutch that decouples the two motions. From Eqs. (8) and (9) and the requirement that $E = E_n + E_c$ is constant, it follows that for linear springs, the mechanism should satisfy

$$x_c = \sqrt{\frac{2E - k_n \max(x_n, 0)^2}{k_c}} \tag{11}$$

Using Eq. (3), the transfer function becomes:

$$h(x_n) = -\frac{k_n}{k_c} \frac{x_n}{\sqrt{\frac{2E - k_n x_n^2}{k_c}}} \tag{12}$$

Fig. 3 shows a schematic explanation of the forces in such a mechanism as function of the position of the braking block. This figure shows that the overall characteristic is equal to zero for $x_n \geq 0$, while the normal force at those positions depends linearly on the position. This means that the actuator does not have to apply any force to maintain a certain normal force between the friction surfaces. Note that in this example, $h(x_n < 0) \neq 0$, meaning that the system is not statically balanced for $x_n < 0$.

The concept of SBBs depends on a decoupling of the normal force between two friction surfaces and the force required to engage or disengage the brake. Without the static balancing, the actuator that moves the braking block would also have to deliver the force that pushes the friction surfaces together. With the static balancing, the braking block can be moved by an actuator that does not have to counteract any spring force (Eq. (7)). This controlled position determines the braking torque (Eq. (2)).

3. Possible embodiments

The previous section presented requirements on mechanisms for SBBs. Theoretically, when satisfying those requirements, a reduction in the actuation force of 100 % can be achieved. In order to design mechanisms that meet those requirements, in this section we categorize mechanisms that are suitable to be used in SBBs. Two of those concepts were built and the results will be shown in the next two sections.

The categorization is limited by three constraints that will lead to mechanisms that have the potential to be small and lightweight. First, we only consider one DOF mechanisms. More DOF mechanisms for SBBs are also possible, but this requires extra components and extra actuators, increasing the size and mass of the brake. Secondly, the type of spring that is used as normal force spring

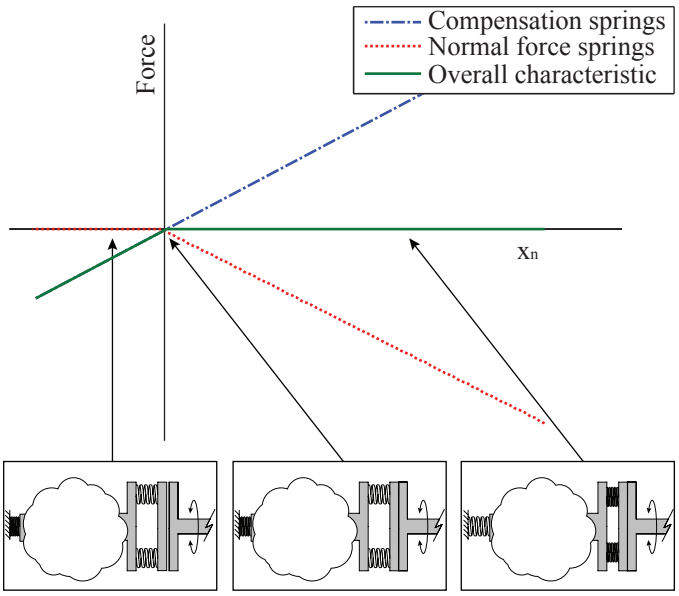

Figure 3: The working principle of a statically balanced brake. The compensation springs have a negative stiffness when measured at the braking block and the normal force springs have a positive stiffness. Since the stiffnesses cancel out and the equilibrium positions coincide, the overall characteristic has a range of zero force, which is the actuation stroke. A small actuator can position the brake at any position in this range, controlling the normal force and thus the braking torque.

or compensation spring should match the type of DOF that it is attached to. For instance, we do not consider mechanisms in which a translational spring is connected to a rotating link. Such a construction does not allow for alignment of spring and the DOF and will therefore lead to an increase in size. Thirdly, we only consider mechanisms with the least amount of components. For instance, a four bar mechanism is considered, but an eight bar mechanism with one DOF is not considered.

In general, mechanisms can be divided into rigid body mechanisms and compliant mechanisms. In rigid body mechanisms, all the parts are rigid except for the springs that are either translational or rotational. For the purpose of this paper, we split rigid body mechanisms into linkage mechanisms and cam mechanisms. The overall categorization of mechanisms is shown in Fig. 4, that also

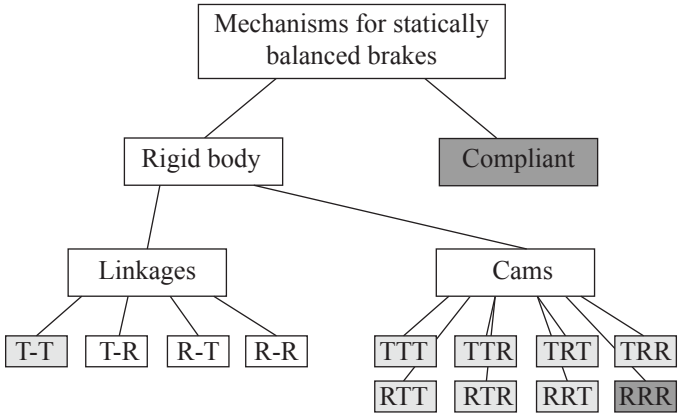

Figure 4: A visualization of the categorization of mechanisms for statically balanced brakes. A first division is made between rigid body mechanisms and compliant mechanisms. Rigid body mechanisms are split into linkages and cam mechanisms. Linkages are categorized based on the nature of their input and output (rotational or translational). One category of linkages leads to a feasible concept. Cam mechanisms are categorized on the nature of their input, output and cam movement (rotational or translational). In the grey categories it is possible to obtain perfect static balance. From the dark-grey categories we show a prototype in this paper.

already shows which categories are feasible. This section first analyses rigid body mechanisms and then compliant mechanisms. This analysis results in a list of feasible concepts and a description of how to construct them.

3.1. Rigid body: Linkages

The first class of rigid body mechanisms for SBBS is linkage mechanisms. In order to categorize one DOF linkages further, we have to realize that the mechanism should at least possess one singular position. This follows from Eq. (10), where the transfer function becomes zero at position $x_n = 0$. This position should be reachable to fully unload the normal force spring to obtain a zero braking torque. Therefore, we categorize both linkage and cam mechanisms further by categorizing singular mechanisms. There exists literature on singular mechanisms and how to categorize them [24, 25, 26]. However, those categorizations are based on different types of mechanical singularities and do not lead

to a complete list of mechanisms. Here we introduce a new categorization that provides such a list and only incorporates simple singular mechanisms, leading to small and lightweight designs. Our categorization of singular mechanisms is based on the notion that all one DOF singular mechanisms have one input motion and one output motion. In simple singular mechanisms, these input and output motions are either translational or rotational motions. In linkages this leads to four categories:

1. translational input - translational output (see Fig. 5a)
2. translational input - rotational output (see Fig. 5b)
3. rotational input - translational output (see Fig. 5b)
4. rotational input - rotational output (see Fig. 5c)

All mechanisms use the same notation. x_n and x_c denote the displacements of the springs and can be rotational or translational. x_i and x_o denote the position of the input and output translations or rotations. l and θ refer to constant distances and angles, respectively. k_n and k_c denote the stiffnesses of the normal force springs and compensation springs. And finally d and γ refer to distances and angles that change when the position of the mechanism changes.

The four categories of mechanisms will be discussed below. Before discussing them, it should be noted that the placement of translational normal force springs becomes impractical when they are both rotating and translating; see for example the left spring in Fig. 5a. Therefore, translational normal force springs can only connect to a slider that is in line with the spring. This also ensures that at a certain position, the force in the normal force springs becomes zero.

3.1.1. Translational input - translational output

A generalized version of this mechanism is shown in Fig. 5a. It consists of two sliders that intersect in O. θ_3 denotes the angle between the two sliders and x_i and x_o denote the positions of the sliders measured from O. The link between the two sliders has length l_3 and each slider connects to a spring. The

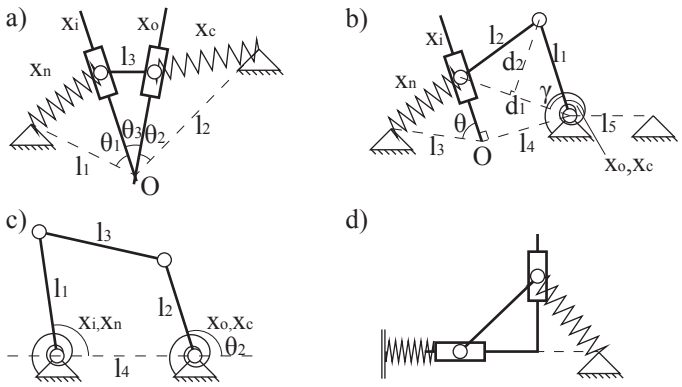

Figure 5: The collection of possible simple singular linkage mechanisms. a) A mechanism with translational input and output. This mechanism can be statically balanced. b) A mechanism with translational input and rotational output. c) A mechanism with rotational input and output. d) A statically balanced version of a.

other sides of the springs are connected to the ground at distances l_1 and l_2 from O under angles of θ_1 and θ_2. Since the left spring should be in line with the left slider, it is given that $\theta_1 = 0$. The energy in the system can be obtained by applying cosine rules:

$$\begin{aligned} x_n^2 =& l_1^2 + x_i^2 - 2l_1 x_i \\ x_c^2 =& l_2^2 + x_o^2 - 2l_2 x_o \cos(\theta_2) \\ l_3^2 =& x_i^2 + x_o^2 - 2x_i x_o \cos(\theta_3) \qquad (13) \\ E =& \frac{1}{2} k_n x_n^2 + \frac{1}{2} k_c x_c^2 \\ E =& C_1 + \frac{1}{2}(k_n - 1)x_i^2 + \frac{1}{2}(k_c - 1)x_o^2 \qquad (14) \\ & + x_i x_o \cos(\theta_3) - k_n l_1 x_i - k_c l_2 x_o \cos(\theta_2) \end{aligned}$$

where C_1 is the constant term:

$$C_1 = l_3^2 + \frac{1}{2} k_n l_1^2 + \frac{1}{2} k_c l_2^2 \qquad (15)$$

We can derive x_o as function of x_i from Eq. (13) and fill it into Eq. (14). Now for static balance, Eq. (4) should hold for all x_i, which is only true when $\theta_2 = \theta_3 = 0.5\pi$, $l_1 = 0$ and $k_n = k_c$. Such a mechanism is depicted in Fig. 5d,

where the ground can be moved freely along the dashed line. The normal force tension spring is changed into a compression spring in this example and is connected to friction plates. The fact that this category leads to a feasible solution is indicated in Fig. 4. The feasible mechanism in this category is not a new mechanism [27]. However, here we proved that this mechanism is in fact the only feasible mechanism in this category.

3.1.2. Translational input - rotational output

A generalized version of this mechanism is shown in Fig. 5b. It consists of one slider with a zero position $x_i = 0$ at O and a crank mechanism with links of lengths l_1 and l_2. One spring is placed between the slider and the ground and the other is placed between the crank and the ground. Since the left spring should be in line with the left slider, it is given that $\theta = 0$. The energy in this system can be derived as follows. First, we define d_2 as the distance between the joint that connects the the two bars of the crank and the line d_1:

$$\begin{aligned} d_2 =& l_1 \cos(\gamma) \\ d_1 =& \sqrt{l_1^2 - d_2^2} + \sqrt{l_2^2 - d_2^2} \\ x_i =& \sqrt{d_1^2 - l_4^2} \\ x_n =& (x_i - l_3) \\ E =& \frac{1}{2} k_n x_n^2 + \frac{1}{2} k_c (x_c - x_{c,0})^2 \end{aligned} \tag{16}$$

where $x_{c,0}$ is the equilibrium position of the rotational spring. Again for static balance, Eq. (4) should hold for all x_i, which is only the case when $k_n = k_c = 0$. Since the stiffnesses should be larger than zero, it is impossible to use this mechanism for a perfectly statically balanced brake, as indicated in Fig. 4. The use of imperfectly statically balanced mechanisms will be discussed in section 6.3.

3.1.3. Rotational input - translational output

This system is the same as the system with translational input and rotational output in Fig. 5b, with the difference that the input and output are switched.

The energy in the system can now be calculated by:

$$\begin{aligned} x_i =& \sqrt{d_1^2 - l_4^2} \\ x_n^2 =& l_3^2 + x_i^2 - 2 l_3 x_i \cos(\theta) \\ E =& \frac{1}{2} k_n x_n^2 + \frac{1}{2} k_c (x_c - x_{c,0})^2 \end{aligned} \tag{17}$$

Since it is impossible to satisfy Eq. (4) with non-zero stiffnesses, it is impossible to perfectly statically balance this system, as indicated in Fig. 4.

3.1.4. Rotational input - rotational output

A generalized version of this mechanism is shown in Fig. 5c. The input and output links and the link in between form a four bar mechanism with lengths l_1, l_2, l_3 and l_4. One rotational spring is placed between link 1 and the ground. The second rotational spring is placed between link 2 and the ground. The energy can be calculated by:

$$E = \frac{1}{2} k_n (x_n - x_{n,0})^2 + \frac{1}{2} k_c (x_c - x_{c,0})^2$$

Again, such a mechanism cannot be perfectly statically balanced, as indicated in Fig. 4.

This leads to the conclusion that the only feasible simple linkage mechanism for SBBs is the one depicted in Fig. 5d.

3.2. Rigid body: Cams

The second class of rigid body mechanisms are cam mechanisms. Cams can be categorized based on the same principle as we used to categorize linkages. Therefore, the normal force spring and the compensation springs can be translational or rotational. However, in cams mechanisms, the cam itself can also be rotational or translational, leading to eight categories (see Fig. 4).

In order to keep the discussion of those categories brief, we discuss the building blocks from which those categories can be constructed (see Figs. 6a-d). Due to the design freedom of cams, all eight categories lead to feasible solutions (as indicated in Fig. 4), although some have clear advantages or disadvantages.

Fig. 6e shows one of the eight classes: a rotational cam, a rotational compensation spring and a rotational normal force spring. Here we discuss the components of such mechanisms, which can be split into:

1. A translational spring on a translational cam (Fig. 6a)
2. A translational spring on a rotational cam (Fig. 6b)
3. A rotational spring on a translational cam (Fig. 6c)
4. A rotational spring on a rotational cam (Fig. 6d)

In the analysis, we make three assumptions for simplicity. Firstly, we assume that the rollers on the cam have a radius of zero. How the analysis changes with a non-zero radius is described in [28]. Secondly, we assume that the grounds at which the springs are connected are in line horizontally with the center of the rotational cam (see Figs. 6b and 6d). Gounds that are not in line are also possible and would add an offset to the equations. Thirdly, we assume that the translational springs are placed horizontally. Translational springs under an angle are also possibe, but would make the analysis unnecessarily complicated.

The notation that is used is as follows. The lengths of the springs are denoted by x_n for the normal force springs and x_c for the compensation springs. $x_{n,0}$ and $x_{c,0}$ denote the equilibrium positions of the springs, meaning that the displacements of the springs are $x_n - x_{n_0}$ and $x_c - x_{c_0}$. x_{cam} denotes the position of the cam, which is translational or rotational. The surface of the cam is obtained in the body fixed workspace coordinates y_1 and y_2. l_1 and l_3 denote the distances between the two grounds and the center of the cam. And finally, l_2 and l_4 denote the length of the links connected to the rotational springs (when present).

In statically balanced cam mechanisms, the cam determines the relationship $x_c = H(x_n)$. Now, x_n can be chosen freely as function of the position of the cam. Then, by filling in Eq. (11), we obtain:

$$x_c(x_{cam}) = \sqrt{\frac{2E - k_n(x_n(x_{cam}) - x_{n,0})^2}{k_c}} + x_{c,0} \tag{18}$$

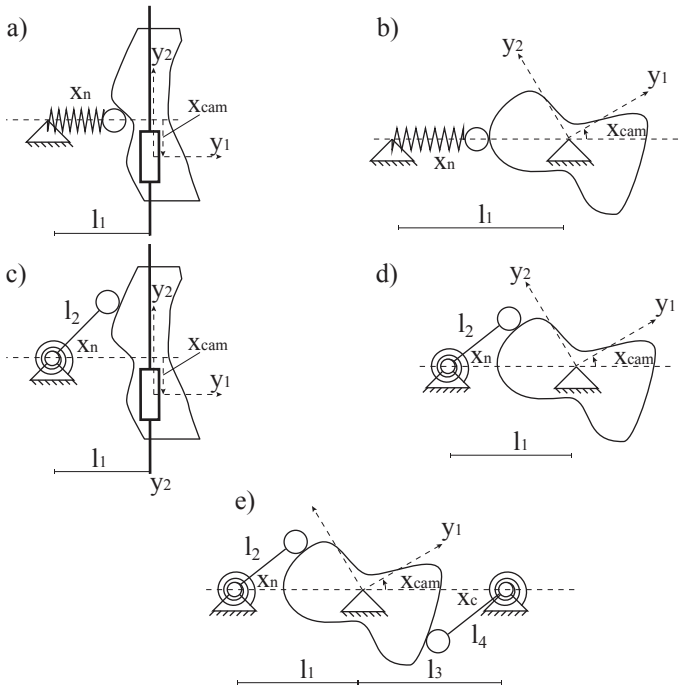

Figure 6: The collection of possible simple cam mechanisms which can be combined to form to SBBs. The mechanisms have rotational or translational inputs, outputs and cams. Combining two simple cam mechanisms to obtain a SBB leads to eight categories: a-a, a-c, c-a, c-c, b-b, b-d, d-b and d-d. e) shows a SBB of configuration c-c.

Using Eq. (18), a trajectory for $x_c(x_{cam})$ can be found as function of the trajectory $x_n(x_{cam})$. Designing a cam now splits into three steps. First, a displacement function $x_n(x_{cam})$ should be chosen. Secondly, using this function the displacement function $x_c(x_{cam})$ can be calculated. And finally, when $x_n(x_{cam})$ and $x_c(x_{cam})$ are known, the cam surface can be obtained in the body fixed workspace coordinates y_1 and y_2. We will now present the equations to obtaining a cam surface with the desired follower behaviour for the four building blocks in Fig. 6. Afterwards, we will give an example that takes all three steps.

3.2.1. Translational spring - translational cam

An example of such a submechanism is shown in Fig. 6a. The shape of the cam surface for the normal force springs in the workspace coordinates y_1 and

y_2 can now be obtained with:

$$\begin{bmatrix} y_1 \\ y_2 \end{bmatrix} = \begin{bmatrix} x_n(x_{cam}) - l_1 \\ x_{cam} \end{bmatrix} \tag{19}$$

This defines the cam surface for the side with the normal force springs. The side with the compensation springs works the same.

3.2.2. Translational spring - rotational cam

An example of such a submechanism is shown in Fig. 6b. The cam shape can be obtained with:

$$\begin{bmatrix} y_1 \\ y_2 \end{bmatrix} = \begin{bmatrix} (x_n(x_{cam}) - l_1)\cos(x_{cam}) \\ (x_n(x_{cam}) - l_1)\sin(x_{cam}) \end{bmatrix} \tag{20}$$

3.2.3. Rotational spring - translational cam

This submechanism is shown in Fig. 6c. The cam shape in body fixed workspace coordinates can be obtained with:

$$\begin{bmatrix} y_1 \\ y_2 \end{bmatrix} = \begin{bmatrix} l_2\cos(x_n(x_{cam})) - l_1 \\ l_2\sin(x_n(x_{cam})) + x_{cam} \end{bmatrix} \tag{21}$$

3.2.4. Rotational spring - rotational cam

A schematic drawing of this submechanism is shown in Fig. 6d. The cam shape can be obtained using the equations:

$$\begin{bmatrix} y_1 \\ y_2 \end{bmatrix} = R(x_{cam}) \cdot \begin{bmatrix} l_2\cos(x_n(x_{cam})) - l_1 \\ l_2\sin(x_n(x_{cam})) - l_1 \end{bmatrix} \tag{22}$$

where $R(x_{cam})$ denotes the rotation matrix for a rotation of x_{cam}.

3.2.5. Cam mechanism example (RRR)

As an example, Fig. 6e shows the mechanism with two rotational springs and a rotational cam. A preliminary study showed that this concept was most promising of all rigid body mechanisms in terms of compactness. Therefore, we also built a prototype of this concept (see section 5). For the analysis we must

first choose a displacement function $x_n(x_{cam})$, the stiffnesses and the equilibrium positions:

$$x_n(x_{cam}) = \sin(x_{cam}) \tag{23}$$

$$k_n = k_c = k \tag{24}$$

$$x_{n,0} = l_1 = x_{c,0}, l_3 \tag{25}$$

From Eq. (18) it follows that the displacement function $x_c(x_{cam})$ is equal to:

$$x_c(x_{cam}) \quad = \quad \cos(x_{cam}) \tag{26}$$

Here we chose a sine as a spring displacement function of the normal force springs, which leads to a cosine in the displacement function of the compensation springs. For every choice for a spring displacement function, a displacement function of the compensation springs exists that leads to a perfectly statically balanced mechanism. The choice for a sine will prove to result in a cam that can rotate 360 degrees. The cam trajectory for both springs is obtained by filling in Eq. (22):

$$\begin{bmatrix} y_{1,n} \\ y_{2,n} \end{bmatrix} = R(x_{cam}) \cdot \begin{bmatrix} l_2 \cos(\sin(x_{cam}))) - l_1 \\ l_2 \sin(\sin(x_{cam}))) - l_1 \end{bmatrix} \tag{27}$$

$$\begin{bmatrix} y_{1,c} \\ y_{2,c} \end{bmatrix} = R(x_{cam}) \cdot \begin{bmatrix} l_4 \cos(\cos(x_{cam}))) - l_3 \\ l_4 \sin(\cos(x_{cam}))) - l_3 \end{bmatrix} \tag{28}$$

There are two options to create this cam surface. Firstly the cam can be split in two halfs where one half connects to the normal force spring and the other half connects to the compensation spring. Secondly the position of the compensation spring can be altered and placed vertically in Fig. 6e. By doing so a 0.5π phase shift is obtained in x_{cam} for the compensation spring trajectory. Since $\sin(x_{cam}) = \cos(x_{cam} - 0.5\pi)$, the same cam surface can be used as for both the normal force spring and the compensation spring. Therefore, the cam is statically balanced for the full 360 degrees. This concept is implemented in the embodiment that will be explained in section 5.

3.3. Compliant mechanisms for SBBs

Instead of having rotational or translational springs and a rigid body mechanism in between, compliant mechanisms could be used. Applying compliant mechanisms varies from using springs with a range of positions with negative stiffness to making the whole mechanism out of one part. Compliant mechanisms are harder to categorize than the rigid body mechanisms earlier in this section.

In their handbook of compliant mechanisms, Howell et al. [29] categorized compliant mechanisms in two ways: based on the used components and based on their application. Here, we only indicate that there is a difference between SBBs with one compliant mechanism that fulfills the function of both the normal force springs and the compensation springs in Fig. 2 and SBBs with a spring with a range of positions with negative stiffness that is used in a configuration with two spring systems. The latter option will be exploited in the embodiment in section 4. Two common types of springs that are known to exibit the capacity to have range of positions with negative stiffness are leaf springs [30] and disk springs (also called Belleville springs) [31].

4. Example 1: Compliant mechanism: bi-stable leaf springs

This section presents the first of two prototypes that were build to verify the performance of SBBs. The prototype in this section has compression springs as normal force springs and leaf springs with a range of positions with negative stiffness as compensation springs (see Fig. 7). This concept has a third group of springs, called the counter springs, to compensate for the non-linear behavior due to disengagement of the friction surfaces in Eq. (8). We chose to build a prototype of this category to illustrate the possibilities and issues of this type of SBBs. The results in this section will show that the actuation force is reduced by 95 % in comparison to a regular brake.

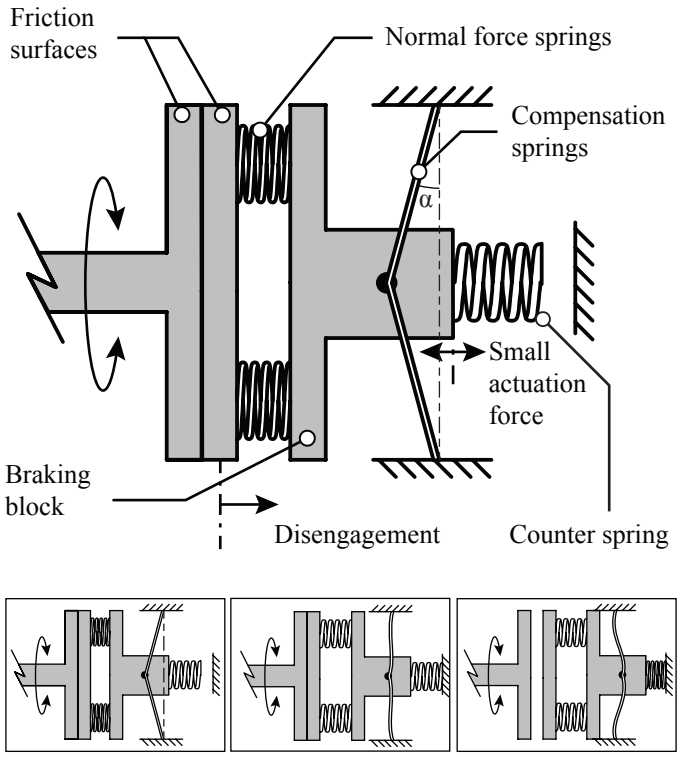

Figure 7: A schematic drawing of the statically balanced brake with leaf springs. The left friction surface is connected to a joint that has to be braked. The right friction surface is connected through the normal force springs with the braking block. The braking block is connected to the ground through leaf springs with a range of positions with negative stiffness and through the counter springs that engage when the friction surfaces disengage. The three configurations at the bottom show how the springs are deformed when the braking block changes position. They show an engaged brake (left), a disengaged brake (right) and a brake that is on the verge of engagement (middle).

4.1. Static balancing

The energy in the normal force springs is given by Eq. (8). The leaf springs with a range of positions with negative stiffness are the compensation springs in this embodiment. In the range with negative stiffness, their energy can be approximated by

$$E_c = \frac{1}{2} k_c x_c^2 + E_0 \tag{29}$$

where k_c is negative and E_0 is a constant. The third group of springs in this embodiment (i.e. the counter springs) engage when the normal force springs disengage. The energy in this spring system is equal to

$$E_{ctr} = \frac{1}{2} k_{ctr} \min(x_{ctr}, 0)^2 \tag{30}$$

where the min operator returns the lowest value of the two inputs. Now if $k_n = k_{ctr} = -k_c$ and $x_n = x_c = x_{ctr}$, the total energy in the system is constant:

$$E = E_n + E_c + E_{ctr} = E_0 \tag{31}$$

4.2. Detailed design

Fig. 8 shows a section view CAD drawing of this embodiment. The amount of positive stiffness of the two groups of compression springs was tuned manually, as will be explained in the next section.

The used friction materials are the specialized friction material Vulka SF-001 and rubber. This leads to a friction coefficient of almost 0.8 and does not lead to sticking behavior. The use of rubber has the disadvantage that rubber tends to wear fast when there is relative movement of the friction surfaces at the moment a normal force is applied. However, in clutches, there should be no relative movement when the device is engaged. If a large amount of relative motion during engagement is to be expected, SF-001 should be used for both friction surfaces, which leads to a friction coefficient of 0.5.

Note that the design of this prototype does not include an actuator, because the main purpose of the prototype is to verify the performance of SBBs and not to be directly implemented in an application. For testing purposes, we connected this prototype to a standard test setup that includes a motor and a loadcell. The same counts for the prototype in section 5.

4.3. Stiffness tuning

The stiffnesses of the three groups of springs have to be balanced. Therefore, we used a leaf spring model in the software package ANSYS$^{\text{TM}}$of which the

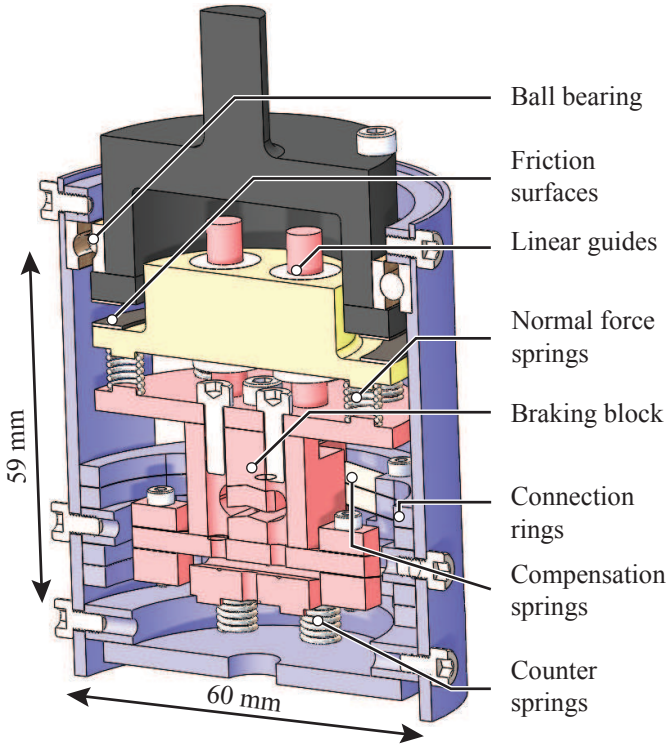

Figure 8: A section view of the embodiment with leaf springs. Parts with the same color (other than grey) are connected and move as one part. The compensation springs (leaf springs) are arranged in eight pairs of two. One side of the leaf springs is connected to the braking block (the red parts), the other side is connected to the ground (the blue parts) through a set of connection rings. The braking block is connected to the bottom friction (the yellow parts) surface by seven normal force springs (compression springs) with a total stiffness of 66.8 N/mm. Four axes that are connected to the braking block are connected to the bottom friction surface through linear ball bearings. These linear guides prevent a torsional load on the normal force springs. At the bottom of the braking block, there is a group of counter springs (compression springs) with a total stiffness of 54.0 N/mm. The top friction surface is connected to the joint (the black part at the top) that has to be braked, which is connected to the ground by a ball bearing. The colors refer to the online version of this article. (For interpretation of the references to color in this figure legend, the reader is referred to the web version of this article.)

correctness was verified in [30]. The used leaf springs are made of stainless steel with an E-modulus of 200 GPa and a Poisson ratio of 0.3. The springs have

Table 1: The parameters of the seven cases

Case	l (mm)	t (mm)	α (deg)	u (mm)
Case 1	10.0	0.10	10.0	0.0
Case 2	10.2	0.10	10.0	0.0
Case 3	10.0	0.11	10.0	0.0
Case 4	10.0	0.10	10.5	0.0
Case 5	10.0	0.10	10.0	0.2
Case 6	10.2	0.09	9.5	-0.05
Case 7	9.8	0.11	10.5	0.2

a width of 7.5 mm, a thickness of 0.1 mm and a length of 10 mm. The angle between the leaf springs and the vertical (see Fig. 7) is $\alpha = 10$ deg. The length and width were chosen to fit in the housing of the brake. The thickness was chosen such that the maximum stress is slightly smaller than the yield strength.

In order to test the sensitivity of the characteristic to manufacturing inaccuracies, we derived the characteristics for one pair of springs with seven slightly different parameter sets (see Table 1). Case 1 uses the intended parameters. In Case 2-5, the length, thickness, angle and pretension were varied. Pre-tension means that the distance between the braking block and the ground is reduced. Then, in Case 6 and 7, the worst and best cases in terms of maximum force were tested.

Fig. 9 shows the seven characteristics. It shows that the characteristic is very sensitive to certain manufacturing inaccuracies. Especially, a pre-tension changes the characteristic drastically. The different parameter variations influence the maximum force, the stroke of the springs and the stiffness.

Since the final characteristic is very sensitive to inaccuracies, we decided to tune the stiffnesses in the final design manually. This tuning consisted of three steps. First we measured the characteristic of the group of leaf springs to determine the amount of positive stiffness k_n and k_{ctr} that should be added, which turned out to be $k_n = 66.8$ N/m and $k_{ctr} = 54.0$ N/m. The two groups

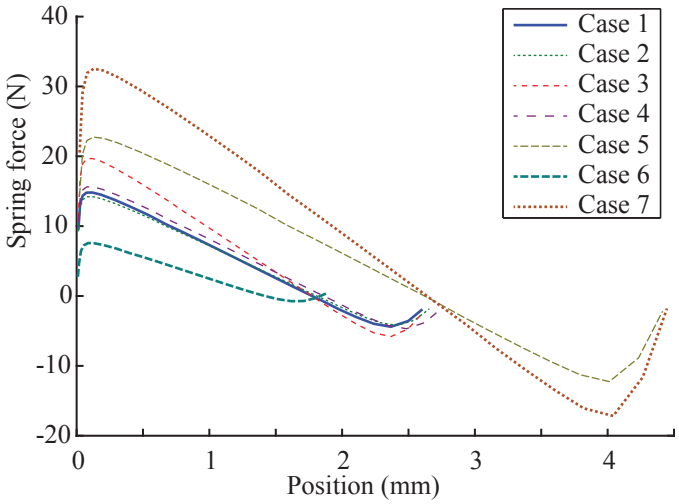

Figure 9: The characteristics of seven sets of springs with slightly varied parameters.

of springs have a different total stiffness in order to better match the sinusoidal-like characteristic of the leaf springs. Second, we added the positive stiffnesses and measured the characteristic again to determine the off-set in x_n and x_{ctr}. Finally, we adjusted the off-sets in x_n and x_{ctr} accordingly and verified the balancing by measuring the overall characteristic. The result of this tuning is presented in the next section.

4.4. Reduction in actuation force

Fig. 10a shows the characteristic of the leaf springs and the tuned characteristic of the three spring systems combined. The maximum actuation force is 5.9N and the maximum normal force is 109.6N. Therefore, the actuation force is reduced with 95% in comparison to a regular brake. The average actuation force within the actuation stroke is 1.83 N, which is an improvement of 97% in comparison to a regular brake.

4.5. Braking characteristic

We measured the braking torque manually at 12 positions by applying torque until the brake starts to slip and thus measuring the static friction. Fig. 10b

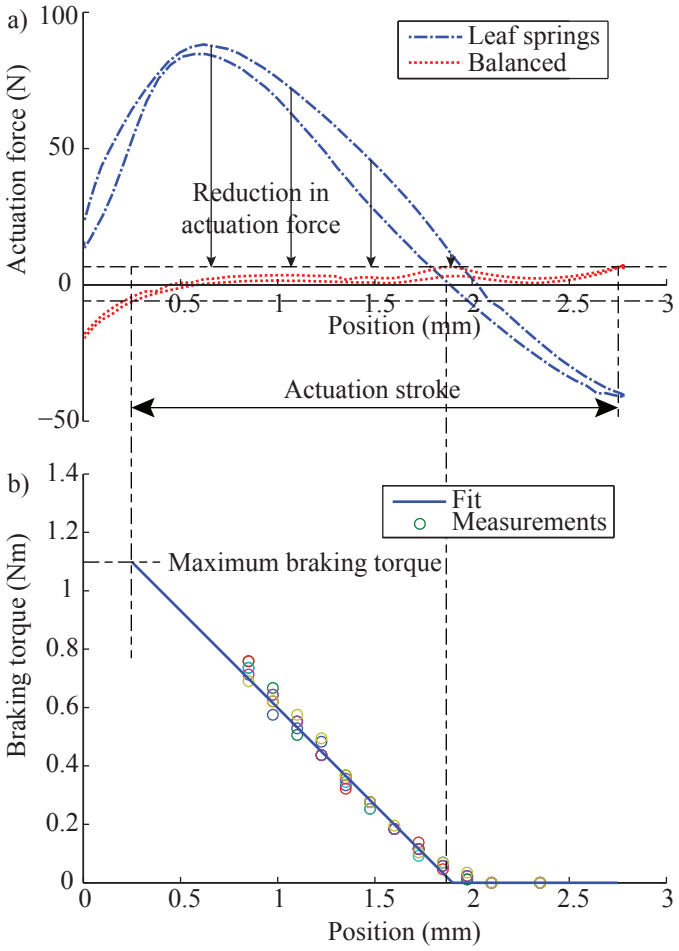

Figure 10: Measurements on prototype 1. a) The characteristics of the leaf springs and the complete statically balanced mechanism. In both cases, the force is measured while moving in both directions. The difference between the two measurements is due to hysteresis. The maximum actuation force is only 5 % of the force in the normal force springs. This means that the actuation force is reduced with 95 % b) The braking torque as function of the position.

shows the braking torque as function of position and the fit through the data. The results show that the braking torque is a piecewise linear function of the position of the braking block. The maximum braking torque is 1.08 Nm.

5. Example 2: Cam mechanisms: RRR

This section shows our prototype of the concept based on a rigid body approach. Rigid body mechanisms have the advantage that they are easier to model than compliant mechanisms. We chose to build a prototype with a rotational cam surface with torsion springs connected to the rotational input and output (see Fig. 6e). The mechanism in Fig. 6e is implemented twice, leading to a total of four torsion springs. An initial case study showed that this concept was most promising in terms of torque density and the results in this section will show that the actuation torque is reduced by 97 % in comparison to a regular brake.

5.1. Detailed design

Fig. 11a shows a CAD drawing of this prototype. The cam shaft is the braking block to which an actuator can be connected. When the cam shaft is rotated, the four followers track the motion induced by the cam surface and the torsion springs are deflected accordingly. The axles running through the followers connect to two components: two connect to the braking arms, the other two connect to the ground. This connection is clarified in Fig. 11b. The axles are connected to the followers through torsion springs with an individual stiffness of 0.64 Nm/rad. The springs are laser cut out of 3mm thick RVS301 spring steel, which has a E-modulus of 189 GPa. The springs have a wall thickness of 1.4 mm and makes 1.75 revolutions.

Fig. 11b depicts the braking side of the mechanism with the brake arms and the friction surface disk of the robot axis. The radius of the friction surface disk is 16mm. Clearly, the robot axis can pass through the entire braking device without obstructions. This has the advantage that this type of brake can also be used in the middle of an axis. The used friction materials are the specialized friction material Vulka SF-001 and rubber (the same as embodiment 1), which have a friction coefficient of 0.8.

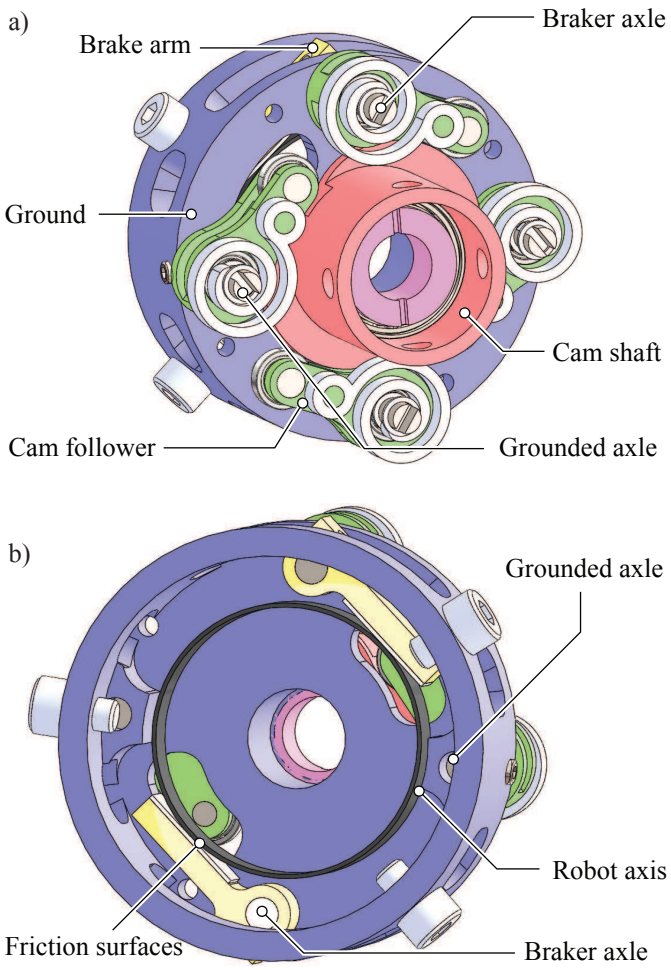

Figure 11: Two CAD drawings of the second embodiment. a) An inside view of the embodiment with torsion springs. b) The back side of the embodiment with torsion springs showing the connection with the braking arms. Four followers (shown in green) roll over the surface of the cam (shown in red). Two connect to the ground (shown in blue) and two connect to the brake arms (shown in yellow). The brake arms then push against a ring on the robot axis (shown in black). (For interpretation of the references to color in this figure legend, the reader is referred to the web version of this article.)

5.2. Reduction in actuation force

Fig. 12 shows both the actuation torque of the cam shaft and the estimated torque in two torsion springs connected to the brake arms. Every 90 degrees,

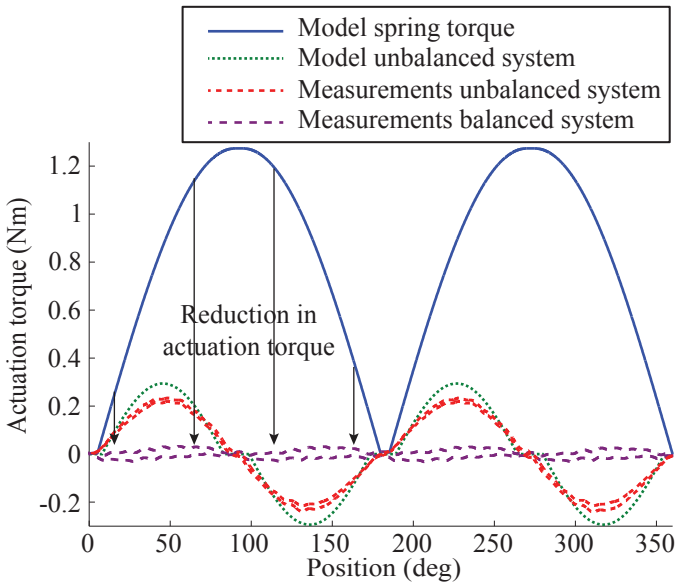

Figure 12: Actuation torque of embodiment 2 for a full rotation of the input cam. The blue solid graph is the estimated torque in the braking springs, the purple dashed graph is the measured input torque. The maximum input torque is only 3 % of the maximum spring torque. This means that the actuation torque is reduced with 97 %.

the system has a singular configuration in which the brake is either fully braking or disengaged. In those singular configurations, the actuation torque is 0 Nm which is a 100% reduction of the torque in the springs. In the non-singular configurations the maximum actuation torque on the cam shaft is 0.04 Nm which is a 97% reduction of the combined actuation torque in the torsion springs connected to the brake arms.

5.3. Braking characteristic

Fig. 13 shows the braking torque as function of the position of the cam. The maximum braking torque in clockwise direction is 0.83 Nm and the maximum braking torque in counter clockwise direction is 0.75 Nm. The cause for this difference is unclear. Part of the difference can be explained by a self-engaging effect similar to that in [5]. For the self-engaging effect to explain the complete difference, the friction force vector should pass the center of the axis of the brake

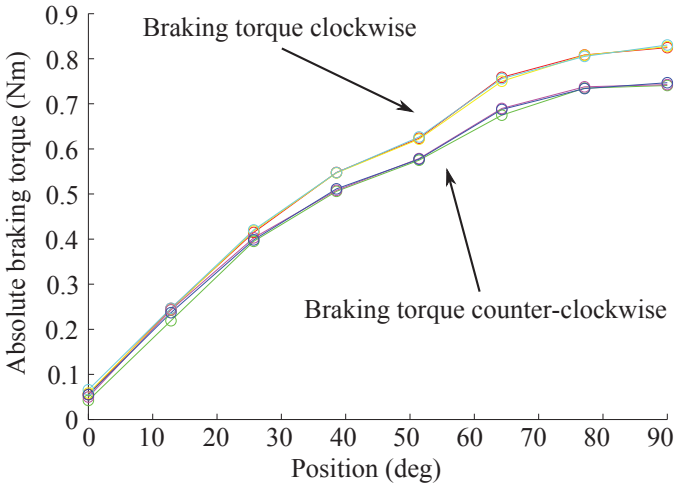

Figure 13: Braking torque of embodiment 2 over a range between 0 degrees (disengaged) to 90 degrees (fully braking) of the cam.

arms at a distance of 0.8 mm. 0.2 mm can be explained by the friction surface that was slightly thicker than anticipated and manufacturing inaccuracies. Another 0.1 mm can be explained by the bending of the brake arms when they apply force on the braking disk. For the remainder of the difference, we do not have an explanation.

Fig. 12 shows the actuation torque for this embodiment when only the two normal force springs are connected. The resulting actuation torque can be used to estimate the actual stiffness of the torsion springs. The calculated maximum input torque was 0.29 Nm and the actual maximum input torque was 0.24 Nm. This leads to the conclusion that the springs have a 20% lower stiffness than expected from the model and the maximum torque the springs produce is 0.64 Nm per spring instead of the calculated 0.80 Nm. Note however, that although the springs do not have the same stiffness as modeled, the brake is still statically balanced as long as the springs are linear.

Table 2: Performance of the embodiments

Criterion	Leaf springs	Rotational cam
Braking torque	1.08 Nm	0.83 Nm
Actuation	5.9 N (= -95%)	0.035 Nm (= -97 %)
Bi-directionality	++	+
Size	∅60x59 mm	∅55x23 mm
Mass	170 g	92 g

6. Discussion

This paper introduced the concept of SBBs, categorized all relatively simple mechanisms that can be used in SBBs and showed two embodiments. The results show that the actuation force/torque can be reduced by 95-97% in comparison to a regular brake. We will now discuss the performance, mechanism selection, the use of imperfectly balanced mechanisms, the energy consumption of SBBs and the applications.

6.1. Performance

Table 2 summarizes the performance of the two embodiments in terms of the braking torque, actuation force/torque, bi-directionality, size, mass. We will now discuss those performance criteria separately. A full comparison between SBBs and other locking mechanisms is provided in [3].

The braking torques of the embodiments are 1.08 Nm, and 0.83 Nm. There are two options to increase the braking torque. The first option is to increase the radii of the friction surfaces and the second option is to increase the stiffnesses of the springs.

The maximum actuation force and torque are 5.9 N and 0.035 Nm for the two embodiments. Since one embodiment has an actuation force and the other has an actuation torque, the two numbers are hard to compare. However, in embodiment 1, the actuation force is only 5 % of the force in the normal force springs and in embodiment 2, the actuation torque is only 3 % of the torque

in the normal force springs. This means that the brakes reach reductions of 95 % and 97 % in comparison to regular brakes. In both cases, the fact that the actuation force is not zero is due to hysteresis and imperfect balancing. Both account for approximately 50% of the maximum actuation force/torque.

For the bi-directionality, we use the qualitative scoring from [3], where $++$ denotes a perfect bi-directionality and $--$ denotes locking only in one direction. The prototype with leaf springs has the same braking torque in both direction and thus scores a $++$. The prototype with a rotational cam has a slightly larger braking torque in one direction and thus it scores a $+$.

The size and mass of embodiment 1 are significantly larger than that of embodiment 2. The challenge in both designs is to miniaturize the mechanism for the compensation springs. In embodiment 1, the leaf springs and their mounting contribute most to mass and size. One possibility to lower the mass and size would be to replace the leaf springs by Belleville springs (also known as disk springs) [31]. More space and mass can be saved by optimizing the design. For example, the braking block, friction surfaces and housing are not optimized for mass and size. In embodiment 2, the cam mechanism and springs are all in one plane, making the design more compact.

6.2. Mechanism selection

In section 3, we categorized all relatively simple mechanisms that can be used between the braking block and the compensation springs. There are no hard rules that, when followed, will automatically lead to the best design. However, here we provide three considerations for selection of a suitable mechanism.

Firstly, rigid body mechanisms in combination with regular springs are easier to model than compliant mechanisms. As shown in section 4, compliant mechanisms can be very sensitive to manufacturing inaccuracies. On the other hand, compliant mechanisms are potentially very compact because the whole mechanism can be made out of one part.

Secondly, rigid body designs are in general smaller when the spring, the actuator and the input and output match. For instance, when a linear actuator

is used, it is inconvenient to connect it to a rotational DOF.

Thirdly, the actuator should not be placed on a joint that can reach a singular position. For instance in Fig. 5b, placing a linear actuator on the vertical slider is not a good idea, because it will not be able to leave the position where the bar is vertical. Instead, a rotational actuator could be placed between the bar and one of the sliders.

6.3. Imperfectly balanced mechanisms

Section 3.1 discusses three categories of linkage mechanisms that cannot be perfectly statically balanced. Therefore, we did not consider them to be applicable. However, these mechanisms can be used when an approximately statically balanced mechanism suffices. Moreover, with imperfectly balanced mechanisms, the different functionalities mentioned in the introduction can be otained: the regular brake, the safety brake and the bi-stable brake. These functionalities can also be obtained in cam mechanisms and compliant mechanisms. Here we explain how these adjustments can be obtained in embodiment 1.

The characteristic in Fig. 10 shows an almost statically balanced mechanism. At positions smaller than 0.5mm, the spring force is negative and at all other positions, the spring force is slightly larger than zero. This means that without any actuation force, the system will move to the 0.5mm position, at which the brake is engaged. This behavior is equal to that of a safety brake: when not actuated, the brake engages.

Changing the zero positions of the normal force or counter springs does not change the stiffness and thus it only shifts the total characteristic up and down. The amplitude of the shift influences the maximum actuation force. When the position at which the counter springs engage with the ground is changed, the behavior can be changed to that of a bi-stable brake. Such a brake has two stable positions: one in which the brake is engaged and one in which the brake is disengaged. When also changing the position at which the friction surfaces engage (and thus effectively changing the zero position of the normal springs), the behavior can be changed to that of a regular brake, which is only braking

when actuated.

6.4. Energy consumption

Throughout this paper we only considered the actuation force and suggested that this relates to the energy consumption. Only considering the actuation force has the advantage that it is independent of the specific actuator that is used. To get an idea of the actual energy consumption, we will now briefly discuss the power consumption of a DC motor as a brake actuator. The power of a DC motor that is standing still is equal to:

$$P = \frac{F_n^2 \cdot R}{n^2 \cdot k_t^2} \tag{32}$$

where R is the motor resistance, n is the transfer ratio from the position of the motor to the position of the brake and k_t is the motor constant. This power consumption goes to zero when the transfer ratio n goes to infinity. However, since this also increases friction, size and mass, this transfer ratio cannot be chosen too large. Now given a certain n, k_t and R, we see that the power consumption scales quadratically with the actuation force. In most other actuators, the energy consumption will scale with the actuation force and therefore, a higher actuation force will result in a higher energy consumption.

There are actuators in which the energy consumption (theoretically) is independent of the actuation force. Examples are electro-static and piezo-electric actuators. However, those actuators have other disadvantages that make them less suitable for application in brakes, as explained in the introduction.

6.5. Applications

The intended application of the brakes we introduced in this paper is robotics. The use of locking devices in robotics is increasing [3]. Such locking devices are mainly used to reconfigure robots, decrease actuator load when standing still, and control the energy release of springs. Especially in mobile robots, such as household robots or walking robots, components that do not consume energy are advantageous.

The main reason for using a SBB in comparison to other brakes is when only a small actuation force is available and the brake should be able to brake in two directions. Other possible applications for statically balanced brakes include torque limiters, cars, trains, buses, trucks and bikes. Especially the safety/parking brake version of the brake that we showed in this paper is applicable in vehicles such as buses and trucks that often use such brakes to stand still.

As stated in [3], brakes are often used as locking mechanisms or clutches. Using a brake as a clutch (instead of quickly switching clutches such as ratchets) has two advantages. Firstly, a brake can disengage while under load and secondly, the braking torque is independent of the position of the joint.

7. Conclusion

In this paper we introduced a new type of brakes: statically balanced brakes. The goal of SBBs is to eliminate the actuation force required in regular brakes. With small adjustments, SBBs can also be used as safety brakes or bi-stable brakes, with a reduced actuation force. We conclude that the concept of SBBs is promising and that the required actuation force can be reduced by 95-97% in comparison to regular brakes. Furthermore, cam mechanisms seem to be the most promising approach for balancing of the two spring systems because of their design freedom and the fact that they are relatively easy to model.

Acknowledgement

This research was sponsored by Technology Foundation STW (project numbers 11282 and 11832)

References

[1] W. C. Orthwein, *Clutches and brakes: design and selection.* CRC Press, 2004.

[2] R. Limpert, *Brake design and safety*, 1992, vol. 120.

[3] M. Plooij, G. Mathijssen, P. Cherelle, D. Lefeber, and B. Vanderborght, "Lock your robot: A review of locking devices in robotics," *Robotics Automation Magazine, IEEE*, vol. 22, no. 1, pp. 106–117, March 2015.

[4] J. Kim and S. B. Choi, "Design and modeling of a clutch actuator system with self-energizing mechanism," *Mechatronics, IEEE/ASME Transactions on*, vol. 16, no. 5, pp. 953–966, 2011.

[5] B. Peerdeman, G. Pieterse, S. Stramigioli, H. Rietman, E. Hekman, D. Brouwer, and S. Misra, "Design of joint locks for underactuated fingers," in *Biomedical Robotics and Biomechatronics (BioRob), 2012 4th IEEE RAS EMBS International Conference on*, June 2012, pp. 488–493.

[6] D. F. B. Haeufle, M. D. Taylor, S. Schmitt, and H. Geyer, "A clutched parallel elastic actuator concept: Towards energy efficient powered legs in prosthetics and robotics," in *IEEE RAS EMBS International Conference 4th on Biomedical Robotics and Biomechatronics (BioRob)*, 2012, pp. 1614–1619.

[7] P. Guarneri, G. Mastinu, M. Gobbi, C. Cantoni, and R. Sicigliano, "Brake energy efficiency," *Journal of Mechanical Design*, vol. 136, no. 8, p. 081001, 2014.

[8] C. G. Peabody and R. W. Roberts, "Automatic parking brake," Feb. 18 1936, uS Patent 2,031,062.

[9] S. L. Kurichh and L. R. Acre, "Air operated spring brake," Dec. 16 1975, uS Patent 3,926,094.

[10] J. H. Arnold, M. D. DeWitt, R. J. Perisho, and W. L. Soucie, "Electronically controlled parking brake system," Jan. 19 1993, uS Patent 5,180,038.

[11] J. K. Parmerlee *et al.*, "Bi-stable brake," 1973, uS Patent 3,741,353.

[12] J. B. Chou, K. Yu, and M. C. Wu, "Electrothermally actuated lens scanner and latching brake for free-space board-to-board optical interconnects," *Microelectromechanical Systems, Journal of*, vol. 21, no. 5, pp. 1107–1116, 2012.

[13] G. Hirzinger, M. Fischer, B. Brunner, R. Koeppe, M. Otter, M. Grebenstein, and I. Schfer, "Advances in robotics: The dlr experience," *The International Journal of Robotics Research*, vol. 18, no. 11, pp. 1064–1087, 1999.

[14] K. Yamatoh, M. Ogura, K. Kanbe, and Y. Isogai, "Piezoelectric brake device," Aug. 8 1989, uS Patent 4,854,424.

[15] M. G. Hanley, G. P. Caliendo, and D. B. Anderson, "Actuator having piezoelectric braking element," Nov. 16 1999, uS Patent 5,986,369.

[16] S. Munir, L. Tognetti, and W. Book, "Experimental evaluation of a new braking system for use in passive haptic displays," in *American Control Conference, 1999. Proceedings of the 1999*, vol. 6, 1999, pp. 4456–4460 vol.6.

[17] M. Laffranchi, N. Tsagarakis, and D. Caldwell, "A variable physical damping actuator (vpda) for compliant robotic joints," in *Robotics and Automation (ICRA), 2010 IEEE International Conference on*, 2010, pp. 1668–1674.

[18] G. J. Tuijthof and J. L. Herder, "Design, actuation and control of an anthropomorphic robot arm," *Mechanism and machine theory*, vol. 35, no. 7, pp. 945–962, 2000.

[19] M. Vermeulen and M. Wisse, "Intrinsically safe robot arm: Adjustable static balancing and low power actuation," *International Journal of Social Robotics*, vol. 2, no. 3, pp. 275–288, 2010.

[20] J. L. Herder, "Development of a statically balanced arm support: Armon," in *Rehabilitation Robotics, 2005. ICORR 2005. 9th International Conference on*. IEEE, 2005, pp. 281–286.

[21] N. Tolou, G. Smit, A. A. Nikooyan, D. H. Plettenburg, and J. L. Herder, "Stiffness compensation mechanism for body powered hand prostheses with cosmetic covering," *Journal of medical devices*, vol. 6, no. 1, 2012.

[22] N. Tolou, V. A. Henneken, and J. L. Herder, "Statically balanced compliant micro mechanisms (sb-mems): Concepts and simulation," in *ASME 2010 International Design Engineering Technical Conferences and Computers and Information in Engineering Conference*. American Society of Mechanical Engineers, 2010, pp. 447–454.

[23] A. G. Dunning, N. Tolou, and J. L. Herder, "A compact low-stiffness six degrees of freedom compliant precision stage," *Precision Engineering*, vol. 37, no. 2, pp. 380 – 388, 2013.

[24] C. Gosselin and J. Angeles, "Singularity analysis of closed-loop kinematic chains," *Robotics and Automation, IEEE Transactions on*, vol. 6, no. 3, pp. 281–290, Jun 1990.

[25] D. Zlatanov, R. Fenton, and B. Benhabib, "Identification and classification of the singular configurations of mechanisms," *Mechanism and Machine Theory*, vol. 33, no. 6, pp. 743 – 760, 1998.

[26] F. Park and J. W. Kim, "Manipulability and singularity analysis of multiple robot systems: a geometric approach," in *Robotics and Automation, 1998. Proceedings. 1998 IEEE International Conference on*, vol. 2, May 1998, pp. 1032–1037 vol.2.

[27] J. L. Herder, "Energy-free systems. theory, conception and design of statically balanced spring mechanisms," Ph.D. dissertation, Delft University of Technology, 2001.

[28] D. Tsay and B. Lin, "Profile determination of planar and spatial cams with cylindrical roller-followers," *Proceedings of the Institution of Mechanical Engineers, Part C: Journal of Mechanical Engineering Science*, vol. 210, no. 6, pp. 565–574, 1996.

[29] L. L. Howell, S. P. Magleby, and B. M. Olsen, *Handbook of compliant mechanisms*. Wiley Online Library, 2013.

[30] A. G. Dunning, N. Tolou, P. Pluimers, L. Kluit, and J. L. Herder, "Bistable compliant mechanisms: Corrected finite element modeling for stiffness tuning and preloading incorporation," *Journal of Mechanical Design*, vol. 134, no. 8, p. 084502, 2012.

[31] J. Almen and A. Laszlo, "The uniform-section disk spring," *Trans. ASME*, vol. 58, pp. 305–314, 1936.